On Convection During Vb-Cyclone Events in Present and Warmer Climate

Mostafa E. Hamouda[1,2], Christian Czakay[1], and Bodo Ahrens[1].

[1]Institute for Atmospheric and Environmental Sciences, Goethe University Frankfurt, Frankfurt am Main, Germany.
[2]Astronomy and Meteorology Department, Faculty of Science, Cairo University, Cairo, Egypt.

Key Points:

- Convection during Vb-events can be detected by applying a diagnostic method on simulations with parameterized convection.
- Around 30% of Vb-cyclone precipitation due to convection in the present climate, which increases to 52% in the warmer climate SSP5-8.5.
- Convective fraction is larger than the average if the Vb-cyclone is associated with an upper level cut-off low pressure system.

Corresponding author: Mostafa E. Hamouda, hamouda@iau.uni-frankfurt.de

Abstract

Summer extreme flooding in Central Europe is often associated with Vb-cyclones which travel through the Mediterranean, then northwards east of the Alps towards Central Europe. Extreme convective precipitation intensities scale with the Clausius-Clapeyron relation under global warming. This study quantifies the importance of convective precipitation during Vb-events in present and in warmer climate by simulating selected Vb-events with convection-permitting grid-spacing. A simple convective precipitation diagnostic is compared against Lagrangian convective cell tracking. The simple method shows skill identifying convective precipitation in coarser simulations with parameterized convection. On average, 30% of precipitation is classified as convective in reanalysis and historical EC-Earth3 driven simulations. This fraction increases to 52% in a warmer climate under SSP5-8.5 scenario. The increase is explained by a frequency increase of the convectively active cut-off low-pressure systems and a doubling of the convective fraction in the less active trough-like Vb-cyclones, suggesting amplified flood risk in a warmer climate.

Plain Language Summary

Summer extreme flooding events in central Europe is often associated with a cyclone track known as Vb-cyclone, i.e. cyclones travelling through the Mediterranean then moving northwards on the eastern flank of the Alps towards central Europe. Convective precipitation (short showery events) results from the high atmospheric instability causing rapid rising motion and the development of thunderstorms. In this study, we find that convective precipitation is on average 30% of the total precipitation during Vb-cyclones, and this fraction increases to 52% in a warmer climate scenario. The consequence of a larger convective fraction is a tendency to more extreme localized precipitation, potentially leading to more intense flood events during Vb-cyclones.

1 Introduction

Extreme flooding is an important topic for climate research, with numerous studies concerning the various properties of extreme precipitation events, such as origin, development, trends and recurrence (Pendergrass et al., 2015; Tandon et al., 2018; Hamouda & Pasquero, 2021; Gimeno et al., 2022). An important flood producing process in the central European region is known as Vb-cyclone event. Such cyclones are first introduced by van Bebber (1891) are defined as cyclones which travel eastwards over the Mediterranean Sea, then turn northeastwards on the eastern flank of the Alps impacting the river-rich central European region with heavy amounts of precipitation (Ulbrich et al., 2003; Rudolf & Rapp, 2002; Stein & Malitz, 2013) (red tracks in figure 1). In the summer half of the year, Vb-cyclones are more important for flooding, since they can be charged with moisture and energy from the warm Mediterranean sea, the moist warm European soil, and the other marginal seas (Krug et al., 2022; Sodemann et al., 2009; Krug et al., 2021).

The general consensus is that the risk of extreme events is increasing due to global warming, since warmer air temperatures accommodates more moisture content at a rate of $7\%/^{\circ}C$ according to Clausius-Clapeyron (CC) relation. In case of extreme precipitation, the scaling follows an even higher rate of $14\%/^{\circ}C$ at sub-daily time scale, causing more frequent and intense extreme precipitation (Molnar et al., 2015; Brisson et al., 2016; Lenderink et al., 2017; Papalexiou & Montanari, 2019; Purr et al., 2021),.

Many case studies are conducted on the influence of Vb-cyclones on extreme European floods. Flood event of August 2002 is an important event, which was marked by a total precipitation of 350 mm within 24 hours at Zinnwald (Ulbrich et al., 2003; Rudolf & Rapp, 2002)), and another case in 2013 with around 405 mm within 96 hours at Aschau-Stein (Stein & Malitz, 2013).

Case studies provide good understanding of the progression of such extreme events, though lacking robust statistics, which hinders drawing generalized conclusions. However, downscaling enough events is computationally very expensive as long as convective scale is concerned. Therefore, research strives to develop various methods, to identify precipitation due to convection mechanisms using lower computational costs (Churchill & Houze, 1984; Tremblay, 2005; Rasp et al., 2016; Poujol et al., 2020).

The aim of the study is to estimate the importance of convective precipitation during Vb-cyclone events in the present and in a warmer climate scenario, by providing enough events for statistical significance. To this end, we use a regional climate model set up with convective-permitting resolution to simulate different Vb-events. Convective cells are then tracked using a Lagrangian tracking method. Moreover, a diagnostic method based on convective precipitation physics to quantify convection is tuned accordingly, and is employed to provide enough statistics to deduce the role of convection process based on a multi-decadal climate simulation of the present and a warmer climate scenario.

2 Data and Methods

2.1 Data

2.1.1 Convection-permitting simulations

The ECMWF reanalysis ERA-5 (Hersbach et al., 2020) was used as forcing data for the convection-permitting simulations (CPS) for 9 selected Vb-events. CPS were performed over the Med-CORDEX domain (Ruti et al., 2016) using COSMO-CLM v5.0 (Consortium for Small-scale Modelling in Climate Mode; Rockel et al. (2008)) ($dx = 0.0275°;\ 3km$) laterally nudged towards the ERA5 reanalysis with a Davis relaxation scheme and hourly updates as recommended in Ahrens and Leps (2021). A short spin-up time of two days is used following Stucki et al. (2020). The parameterization of deep convection was turned off for the CPS and the shallow convection was parameterized after Tiedtke (1989). Moreover, we applied a one-moment microphysics scheme including graupel, following the recommendation of Brisson et al. (2016) to improve the representation of deep convection (Purr et al., 2019, 2021).

2.1.2 ERA-Interim and EC-Earth3 downscaling

The used reanalysis data in this study was ERA-Interim (Dee et al., 2011) dynamically downscaled using COSMO-CLM v5.0 regional climate model (Rockel et al., 2008). In this part, COSMO-CLM (CCLM) was interactively coupled with the ocean model NEMO (Nucleus for European Modeling of the Ocean; (Gurvan et al., 2022)) in the Mediterranean Sea. Freshwater inflow of rivers into the Mediterranean Sea (except for the Nile) was implemented with the river routing model TRIP (Total Runoff Integrating Pathways; (Oki & Sud, 1998)). Model data for historical and warm climate scenarios are obtained from EC-EARTH-Veg 3 CMIP6 (the Coupled Model Intercomparison Project phase 6, (Döscher et al., 2022)) realization r12i1p1f1. The historical climate scenario is from 1951 till 2014, and the warm climate simulation follows the Shared Socioeconomic Pathways SSP5-8.5 (Riahi et al., 2017) from 2015 till 2099. The domain was is the extended Euro-CORDEX (Giorgi et al., 2008) using a horizontal grid-spacing of about 12 km ($dx = 0.11°$). The downscaled ERA-Interim using the coupled system is referred to as CCLM-ERAI, and the downscaled EC-Earth-Veg 3 is CCLM-EC3 (historical and SSP5-8.5) throughout the study. More details about the setup of the coupled model system are given in Primo et al. (2019).

For comparison with the convection-permitting downscaling of single events in section 2.1.1, a similar setup of CCLM (i.e. 12 km with parameterized convection) was used,

except that in this case, without coupling to the ocean model. The forcing data is ERA5 reanalysis, for consistency with section 2.1.1.

2.2 Methods

2.2.1 Vb-cyclone detection and tracking

The method for cyclone tracking used in this study is based on Hofstätter and Chimani (2012) and Hofstätter et al. (2016) and was adapted by Krug et al. (2020). The first step: low pressure systems are detected using the sea level pressure (SLP). Additionally a discrete cosine filter (Denis et al., 2002) was applied to remove spurious minima. The second step: the horizontal wind fields on the SLP and the 700 hPa pressure levels are used to predict the location of the cyclone center for the next time step as a first guess. The third step: the cyclone center closest to the position of the first guess is assigned to the cyclone path. For further details about the tracking algorithm refer to Hofstätter and Chimani (2012) and Hofstätter et al. (2016).

Here, the tracking algorithm is applied with the configuration in Krug et al. (2020). For the tracking the CCLM-ERAI and CCLM-EC3 were remapped to a 0.25° longitude-latitude grid. The tracking was performed within −5° E to 35° E and 26° N to 70° N using a 3-hourly temporal resolution. Cyclones with a lifetime shorter than 24 h were discarded. Following the definition of Hofstätter and Blöschl (2019) all cyclones that crossed the 47° N latitude between 12° E and 22° E while propagating to the northeast were categorized as Vb-cyclones.

2.2.2 Convective precipitation fraction

Two methods are used to detect convective precipitation. The first is following Purr et al. (2019), which is Convective Cell Tracking (CCT) using Lagrangian dynamics. Contiguous precipitation areas with precipitation rate $> 8.5mm/h$ within 5 minutes time step, are considered a potential convective cell. Wind data is used to predict the position of the convective cell at the subsequent time step using a "cone of detection" for each grid point. If a new cell is present in the cone, a probability value is assigned to the origin pixel of the cone, which links this pixel to the new cell.

The second method is following Poujol et al. (2020). This diagnostic method (POJ) is based on vertical velocity and mid-tropospheric vorticity created by convective plumes. This method is adopted here as it shows skill detecting convection, most importantly in mountainous regions, which is an important criteria for our domain and purpose of study. The thresholds are following Poujol et al. (2020) with slight changes given the different horizontal grid-spacing of our simulation. The lower limit of vertical velocity at 500 hPa is 0.05 cm/s, and the upper limit (before lifting is considered topographic) is 0.12 cm/s (0.2 cm/s in Poujol et al. (2020)). The mid-tropospheric vorticity is unchanged ($1.7\times 10^{-4}\ s^{-1}$). A change of the velocity thresholds by ±0.02 m/s does not influence the results substantially. The CPSs are regridded to a 12-km grid similar to that of the parameterized convection simulation before applying POJ method, to tune the thresholds for the decadal-climate simulation. More details about the method and validation are provided in Poujol et al. (2020)

2.3 Hierarchical clustering

To group similar synoptic patterns based on GPH anomalies at 500 hPa, hierarchical clustering approach is adopted similar to Totz et al. (2017). For Vb-cyclone event, 500 hPa GPH anomalies at lag -2 days are recorded as a single vector data point. The algorithm generates a hierarchy of clusters by merging one pair of nearest data points or clusters of points at each step (Wilks, 2011). Clustering is stopped when the distance

between different clusters does not change significantly (nearly constant distance as the number of clusters increase).

3 Results and Discussion

3.1 Convective precipitation during Vb-cyclones

Figure 1a shows the average precipitation associated with Vb-cyclones and the detected tracks in CCLM-ERAI from 1979 till 2014 during the summer half of the year from April till September (AMJJAS).

Studying this particular cyclone track is important as it is associated with extreme precipitation events. The top 5% of extreme precipitation rates are ranked in figure 1b for precipitation within the dashed black box in panel a, demonstrating the occurrence of extreme precipitation in association with Vb-cyclones (red circles). A sample of 9 extreme Vb-cyclone events are selected for convective-permitting scale (CPS) downscaling using CCLM at 3 km (section 2.1.1), and are downscaled using parameterized convection (section 2.1.2). To detect convective precipitation, CCT following Purr et al. (2019) and a diagnostic method (POJ) following Poujol et al. (2020) are used (section 2.2.2).

Figure 2a shows the time evolution of total precipitation, convective precipitation and convection fraction using CCT for July 2008, area-averaged over the Danube catchment (dashed magenta box in figure 1a). Figure 2b is similar to panel (a), except that convective precipitation is detected using POJ method. The two methods exhibit similar patterns of convective fraction with a correlation coefficient CC(a,b)=0.76. It is noted that the timing of the maximum convective rainfall shows a predominant daily cycle, with a main peak during the afternoon, as deep convection is initiated by solar radiation heating the surface, destabilizing the atmospheric boundary layer (Purr et al., 2021). The first peak of convection is particularly high, coinciding with surface air temperature peak (red line in figure 2a), which is attenuated as the event evolves by cloud radiative cooling.

Another lower resolution CCLM simulation with parameterized convection at 12 km is carried out for the same event (figure 2c). The detection of convection was done similarly as in figure 2b using POJ method. Some differences in the total precipitation pattern with respect to the CPS simulation are expected, since different simulation setup was utilized. However, the convective fraction shows similar patterns as indicated by CCT. The other events are shown in the supplementary materials (Figures S1-9).

Comparing POJ method, which does not require high computational power, with the computationally expensive CPS simulations with Lagrangian CCT, shows that it can be applied widely to as many events as possible in our data sets. Furthermore, it is important to highlight that only using the output of model's convection parameterization can lead to overestimation of convection fraction as displayed in Figure S10, while POJ method shows a better representation, even at 12 km resolution.

In closing this section, it is worth mentioning that a counterexample is also carried out, to test the methods ability during seasons where convection is not expected to be as important. Figure S9 shows a Vb-cyclone event in November 2019, just around the beginning of winter, during which convection is not a dominant mechanism for precipitation. The method was able to indicate the absence of convection during this event, which further supports the validity of the method.

3.2 The synoptic setup of strong and weak convective events

Studies show that the frequency of Vb-cyclone events varies between 3-5 cyclones per year (cf. Hofstätter and Chimani (2012); Messmer et al. (2015)), and a more frequent

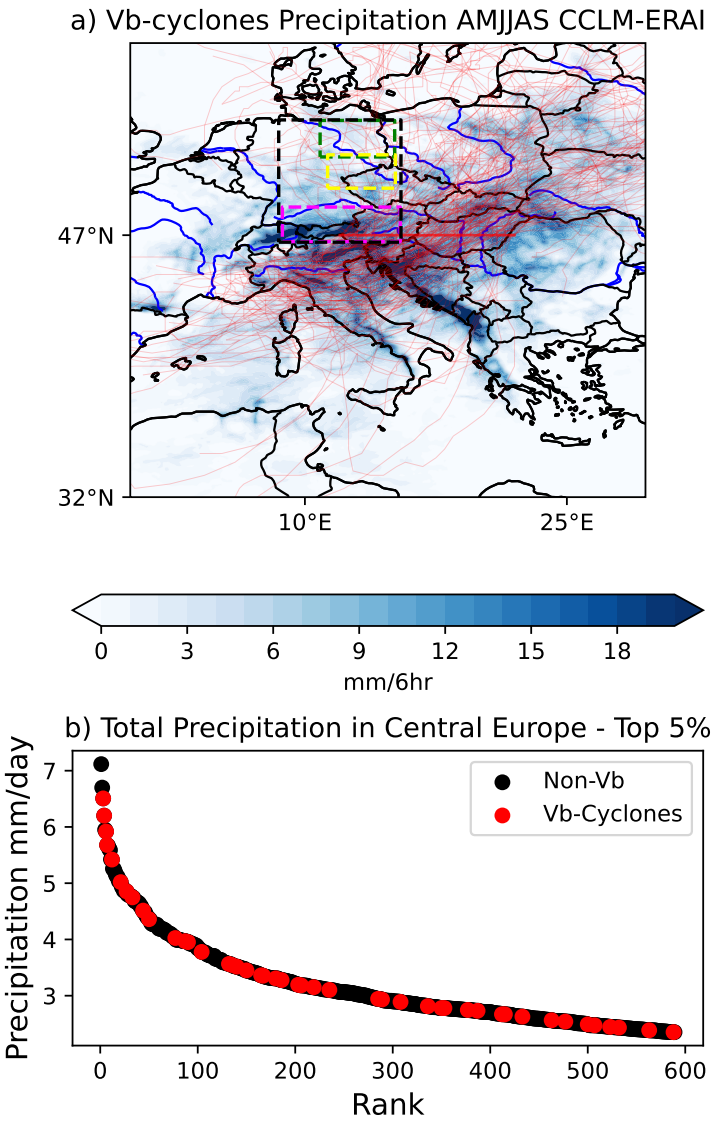

Figure 1. Mean precipitation rate during Vb-cyclones (shading mm/6hr), and detected tracks of pressure minima during the event (red transparent lines) using CCLM-ERAI in the summer half of the year (AMJJAS) from 1979 till 2014. Red line at $47°N$ marks the onset of Vb-cyclone (day 0). Dashed boxes are: Green: Elbe catchment, yellow: Ore catchment, magenta: Danube catchment and black: central Europe. b) Ranking of the top 5% ranked daily precipitation for the central European domain (black dashed box in panel a). Black circles are events not associated with Vb-cyclones, red circles are events associated with Vb-cyclones. Ratio of red to black is 0.11 within the top 100-ranked events.

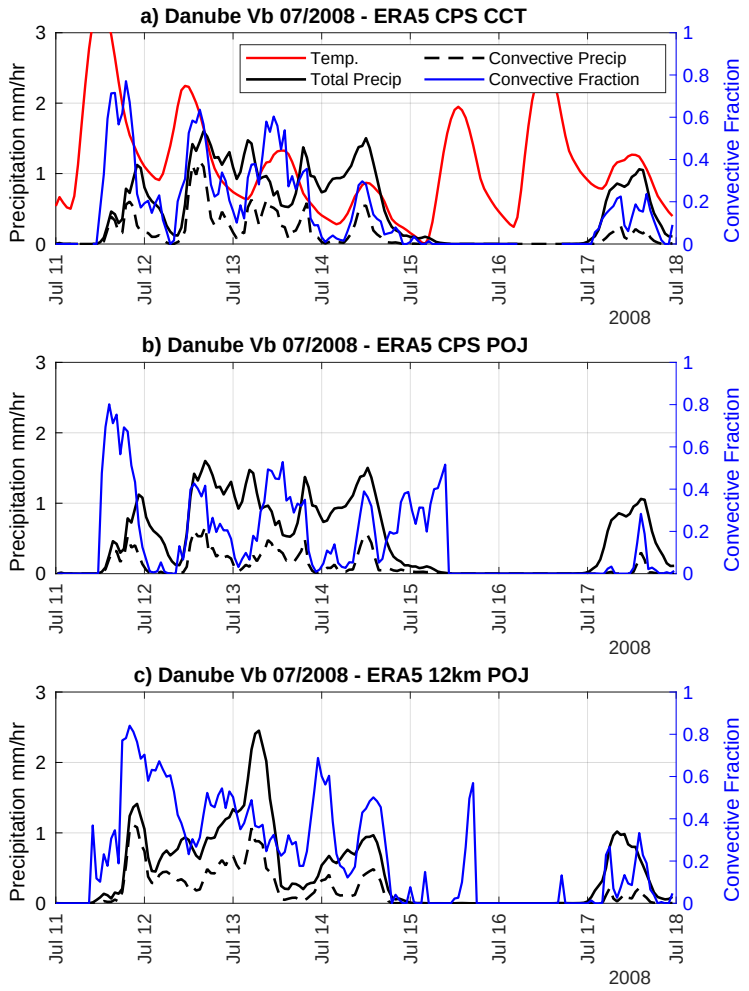

Figure 2. Time series of July 2008 Vb-cyclone as downscaled by COSMO-CLM using ERA5 in the Danube catchment (dashed magenta box in figure 1). a) Downscaled to 3 km (convective permitting simulation; CPS) and tracking convection using CCT. b) Downscaled as in (a), however convection is detected by POJ. c) Downscaled to 12 km (parameterized convection), and convection is detected similar to panel (b). Red line is the time series of surface temperature (arbitrarily scaled).

rate of around 10 cyclones per year in Hofstätter and Blöschl (2019), depending on the quality of the used data set and the rigidity of the definition of the cyclone path. In this study, as described in section 2.2.1, we found 91 cyclones within the period 1979-2014 from April to September (AMJJAS), using the CCLM-ERAI dataset. In this section, we pose the question of how Vb-cyclones differ from the synoptic point of view in the associated convective precipitation, potentially leading to flooding events. Similar to Messmer et al. (2015), where Vb-cyclones are differentiated based on the total amount of associated precipitation. Here our differentiation is based on convection fraction. POJ is employed for the 91 events, and for each event convection fraction is calculated within the dashed black box in figure 1a. The highest and lowest 10% of convection fraction among these events are found to have the thresholds of 0.4 and 0.14 respectively, forming two composites of the synoptic conditions that are associated with strong/weak convective activity during different Vb-cyclones.

Figure 3 shows composites of 500 hPa geopotential height (GPH) anomalies and surface air temperature anomalies 3 days before a Vb-cyclone crosses northwards of $47°N$. High convective activity is associated with Vb-cyclones that are characterized by a cut-off low (COL) pressure system east of the Iberian peninsula, which travels eastwards and then northeastwards to central Europe, while weak convection activity is found during Vb-cyclones moving as a North Atlantic/European trough, extending southwards, possibly becoming cut-off at a later stage. Figures S(11,12) show similar composites for (-2,0) lags.

A high convective event is preceded by ridging (possibly blocking) over central Europe, causing the transport of southeasterly warm continental winds, warming up the central European region of interest as shown in figure 3c. The persistence of such warm anomalies (amplified at lag -2 days in figure S11c) allows the development of a sharp temperature gradients at the frontal zone during the onset of the Vb-cyclone (figure S12c). This result complements the analysis done by Ruff and Pfahl (2023); Ferreira (2021) in which it was shown that extreme total precipitation is associated with upper level COLs. With the transport of moisture from various sources around the cyclone (Krug et al., 2022), such a synoptic setup permits the advection of cold air that is associated with the cyclone, availing significant amounts of convective potential energy.

In contrast, low convection events start by North European troughing (figure 3b), gradually transporting cool northerly air superimposed by the radiative cooling by cloud cover as shown in figure 3d. Further cooling is evident as the trough expands southwards as shown in figures S(11,12)d. This synoptic setting differs with respect to that of a strong convection in that the preceding cooling down of central Europe before the onset of Vb-cyclone significantly dampens the availability of convective energy. The two patterns potentially allow the prediction of whether the Vb-cyclone is set up for a strong or weak convective precipitation.

A caveat of this analysis is the low number of events (highest and lowest 10% of 91 events). However, a similar composite is analysed for a longer data set of CCLM-EC3 in the historical scenario in the period 1951 to 2014 (More details in section 2.1.2). In this dataset, more Vb-cyclones are detected (282 events), and the composites are shown for the highest and lowest 10% of the events (28 events) in figure S13, which confirmed the results.

3.3 Stronger convection in a warmer climate

Extreme precipitation due to convection is particularly important in the context of a warming climate since extreme sub-daily precipitation scales with the CC relation (Lenderink et al., 2017; Purr et al., 2021). The aim of this section is to show the change of convection process within Vb-event under global warming.

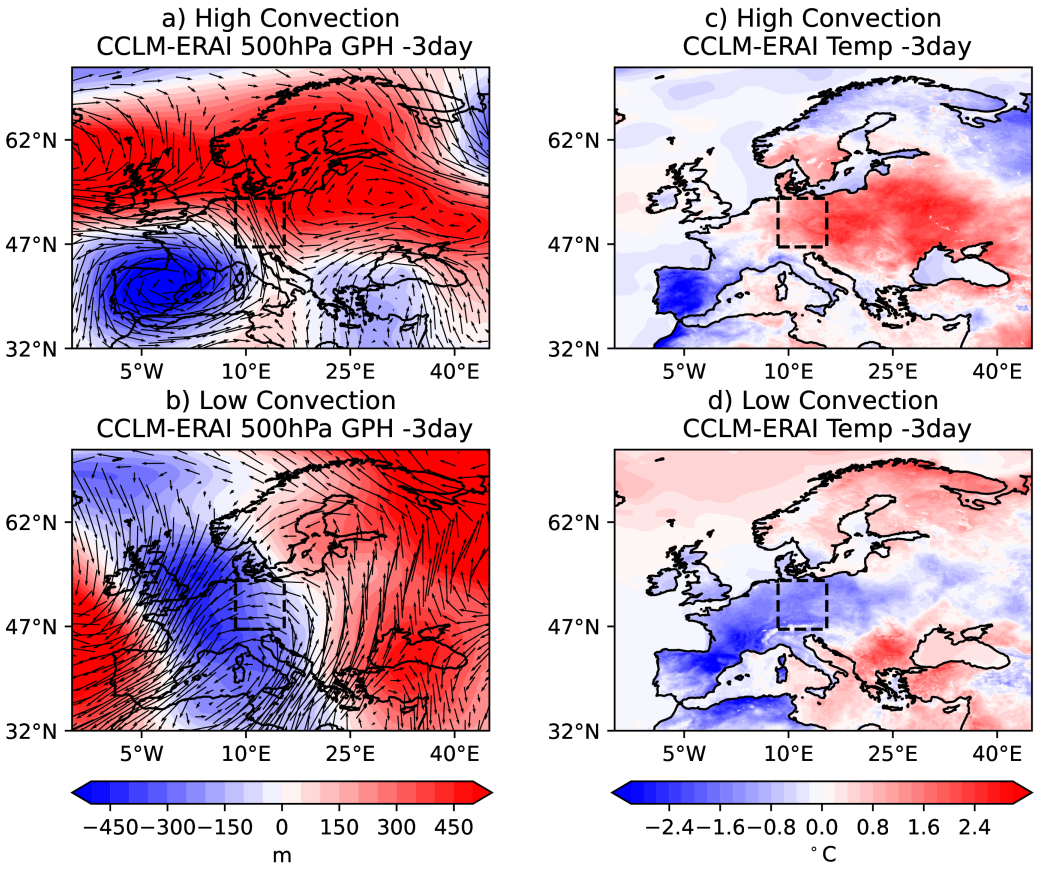

Figure 3. Composites of 500 hPa geopotential height and wind anomalies (shading in meters, and quivers; left column), and surface air temperature anomalies ($^{\circ}C$; right column) 3 days before the onset. Composites are averaged over events with the highest and lowest 10% of convection fraction in CCLM-ERAI as detected by POJ within the dashed black box in central Europe. High convection events with a threshold > 0.4 are in the top row. Low convection events with threshold < 0.14 are in the bottom row.

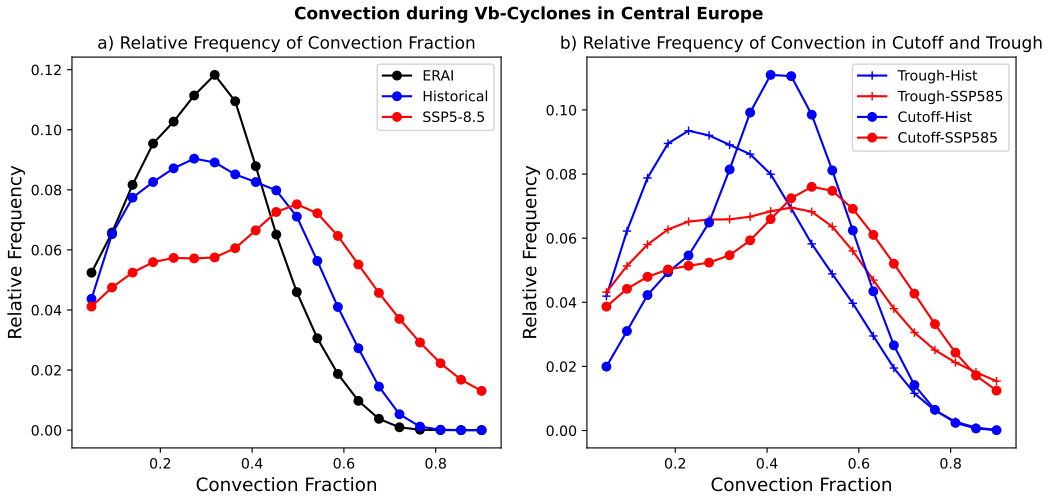

Figure 4. a) The relative frequency distribution for convection fraction within the dashed black box in figure 1 for CCLM-ERAI and CCLM-EC3 (Hist,SSP585). b) similar to panel a, however after clustering to Troughs and COLs in historical and SSP5-8.5.

Figure 4a shows the relative frequency distribution of convection fraction during Vb-events. The fraction is calculated as the average convective precipitation rate as indicated by POJ method divided by the average total precipitation rate during a window of 3 days centered around the peak of maximum precipitation within the dashed black box in figure 1a. The results of CCLM-ERAI and the historical data of CCLM-EC3, show that the convection fraction with the highest relative frequency is around 0.3. In a warmer climate under SSP5-8.5 scenario, the maximum frequency shifts to a higher convection fraction of 0.52, indicating that convection becomes a more dominant precipitation mechanism. This is consistent with the shift in rainfall type from large scale to convective rainfall under warmer temperatures (Lenderink & Meijgaard, 2008; Härter & Berg, 2009).

It is useful to further deduce whether the increasing convection fraction in a warmer climate results from the thermodynamical consequences of CC-relation or due to changes in large scale dynamics such as increasing COL frequency. To distinguish between the two mechanisms, clustering analysis is performed on the spatial pattern of Vb-cyclones in historical and SSP5-8.5 periods, to divide Vb-cyclones into trough and COL events (further details in sec. 2.3).

The outcome of clustering is showing in figure S14, which indicates similar features of troughs and COLs shown in figure 3. In the historical scenario of CCLM-EC3, clustering shows that trough-like Vb-cyclones cover 63% of the events, while the rest are COL-like structure. These percentages change in the warmer climate scenario of SSP5-8.5 to roughly 50-50%.

Figure 4a is reproduced in panel b for each cluster in different scenarios to isolate the thermodynamical and dynamical effects. Figure 4b shows that if the increase of the frequency of COLs is isolated by analyzing only trough-like Vb-cyclones, the most frequent of convection fraction doubles from 0.21 presently to 0.45 in the warmer climate. On the other hand, the most frequent convection fraction of COL-like Vb-cyclones increases from 0.43 up to 0.52. The results suggest that the thermodynamical contribution following CC-relation plays an important role, ruling out the dynamical effect of the increasing COL frequency (summary in table 1).

Table 1. Summary of changes in cluster sizes and convection fraction in CCLM-EC3 historical and SSP5-8.5 scenarios.

	Cluster Size		Convection Fraction	
	COL	Trough	COL	Trough
Historical	37%	63%	0.43	0.21
SSP5-8.5	50%	50%	0.52	0.45

4 Conclusion

Dynamical downscaling is used to investigate the importance of convection during one of the most important cyclones for central Europe, known as Vb-cyclones. First, we evaluate with convection-permitting simulations a diagnostic for convective precipitation presented by Poujol et al. (2020), which is applicable to computationally less expensive simulations with parameterized convection. Second, multidecadal simulations are investigated.

The results show that, on average 30% of Vbs' precipitation is diagnosed as convective in present climate. This percentage increases to 52% in a simulated warmer climate. Thus, precipitation in the warmer climate is more localized and intense during Vb-events. A positive fraction change is expected from the thermodynamical CC relation.

Furthermore, strong convection is associated with cut-off Vb-cyclones travelling over the Mediterranean, setting up sharp surface temperature gradients in central Europe. Weakly convective Vb-cyclones result from Northern Europe troughs. In the warmer climate simulation, cut-off lows were 35% more frequent. Thus, not only the thermodynamical CC process but also the change in large-scale dynamics are important for the change of the convective precipitation fraction.

Our results suggest higher flood risk through more convective precipitation during Vb-cyclone events but are based on one climate realization only. It is therefore encouraged to diagnose an ensemble of climate simulations to improve the robustness of our results.

Open Research ERA5 reanalysis is available on https://cds.climate.copernicus.eu/cdsapp#!/dataset/reanalysis-era5-single-levels?tab=form. CMIP6 data is available on https://esgf-node.llnl.gov/search/cmip6/. Namelists for Downscaling ERA5 to CPS and CMIP6, clustering function, Vb-tracks and Poujol method are provided in the zenodo repository with DOI https://doi.org/10.5281/zenodo.8283417.

Acknowledgments
The financial support of the German Research Foundation (Deutsche Forschungsgemeinschaft, DFG) for the research group FOR 2416 "Space-Time Dynamics of Extreme Floods (SPATE)" (project number 278017089) is gratefully acknowledged. This work used resources of the Deutsches Klimarechenzentrum (DKRZ) granted by its Scientific Steering Committee (WLA) under project 1064. The author sincerely thanks Christopher Purr and Amelie Hoff for providing the setup of CPS and CCT, and Moritz Kirschner for the setup of CCLM-EC3.

References

Ahrens, B., & Leps, N. (2021). Sensitivity of convection permitting simulations to lateral boundary conditions in idealized experiments. , *13*(12).
Brisson, E., Demuzere, M., & van Lipzig, N. P. (2016, 05). Modelling strategies

for performing convection-permitting climate simulations. *Meteorologische Zeitschrift*, *25*(2), 149-163.

Churchill, D. D., & Houze, R. A. (1984). Development and structure of winter monsoon cloud clusters on 10 december 1978. *Journal of Atmospheric Sciences*, *41*(6), 933 - 960.

Dee, D. P., Uppala, S. M., Simmons, A. J., Berrisford, P., Poli, P., Kobayashi, S., ... Vitart, F. (2011). The ERA-Interim reanalysis: configuration and performance of the data assimilation system. *Quarterly Journal of the Royal Meteorological Society*, *137*(656), 553-597.

Denis, B., Côté, J., & Laprise, R. (2002). Spectral decomposition of two-dimensional atmospheric fields on limited-area domains using the discrete cosine transform (dct). *Monthly Weather Review*, *130*(7), 1812 - 1829.

Döscher, R., Acosta, M., Alessandri, A., Anthoni, P., Arsouze, T., Bergman, T., ... Zhang, Q. (2022). The ec-earth3 earth system model for the coupled model intercomparison project 6. *Geoscientific Model Development*, *15*(7), 2973–3020.

Ferreira, R. N. (2021). Cut-off lows and extreme precipitation in eastern spain: Current and future climate. *Atmosphere*, *12*(7).

Gimeno, L., Sorí, R., Vázquez, M., Stojanovic, M., Algarra, I., Eiras-Barca, J., ... Nieto, R. (2022). Extreme precipitation events. *WIREs Water*, *9*(6).

Giorgi, F., Jones, C., & Asrar, G. (2008, 11). Addressing climate information needs at the regional level: The cordex framework. *WMO Bull*, *53*.

Gurvan, M., Bourdallé-Badie, R., Chanut, J., Clementi, E., Coward, A., Ethé, C., ... Moulin, A. (2022, March). *Nemo ocean engine.* Zenodo. doi: 10.5281/zenodo.6334656

Hamouda, M. E., & Pasquero, C. (2021). European extreme precipitation: The effects of spatio-temporal resolution of the data. *Weather and Climate Extremes*, *33*, 100337.

Hersbach, H., Bell, B., Berrisford, P., Hirahara, S., Horányi, A., Muñoz-Sabater, J., ... Thépaut, J.-N. (2020). The era5 global reanalysis. *Quarterly Journal of the Royal Meteorological Society*, *146*(730), 1999-2049.

Hofstätter, M., & Chimani, B. (2012, 10). Van bebber's cyclone tracks at 700 hpa in the eastern alps for 1961-2002 and their comparison to circulation type classifications. *Meteorologische Zeitschrift*, *21*(5), 459-473. Retrieved from `http://dx.doi.org/10.1127/0941-2948/2012/0473` doi: 10.1127/0941-2948/2012/0473

Hofstätter, M., & Blöschl, G. (2019). Vb cyclones synchronized with the arctic-/north atlantic oscillation. *Journal of Geophysical Research: Atmospheres*, *124*(6), 3259-3278.

Hofstätter, M., Chimani, B., Lexer, A., & Blöschl, G. (2016). A new classification scheme of european cyclone tracks with relevance to precipitation. *Water Resources Research*, *52*(9), 7086-7104.

Härter, J. O., & Berg, P. (2009). Unexpected rise in extreme precipitation caused by a shift in rain type? *Nature geoscience*, *2*(6), 372-373.

Krug, A., Aemisegger, F., Sprenger, M., & Ahrens, B. (2022, April). Moisture sources of heavy precipitation in Central Europe in synoptic situations with Vb-cyclones. *Climate Dynamics*.

Krug, A., Pothapakula, P. K., Primo, C., & Ahrens, B. (2021, 07). Heavy Vb-cyclone precipitation: a transfer entropy application showcase. *Meteorologische Zeitschrift*, *30*(3), 279-284.

Krug, A., Primo, C., Fischer, S., Schumann, A., & Ahrens, B. (2020, 08). On the temporal variability of widespread rain-on-snow floods. *Meteorologische Zeitschrift*, *29*(2), 147-163.

Lenderink, G., Barbero, R., Loriaux, J. M., & Fowler, H. J. (2017). Super-clausius–clapeyron scaling of extreme hourly convective precipitation and its relation to large-scale atmospheric conditions. *Journal of Climate*, *30*(15),

6037 - 6052.

Lenderink, G., & Meijgaard, E. (2008, 07). Increase in hourly precipitation extremes beyond expectations from temperature. *Nature Geoscience - NAT GEOSCI*, *1*, 511-514.

Messmer, M., Gómez-Navarro, J. J., & Raible, C. C. (2015). Climatology of vb cyclones, physical mechanisms and their impact on extreme precipitation over central europe. *Earth System Dynamics*, *6*(2), 541–553.

Molnar, P., Fatichi, S., Gaál, L., Szolgay, J., & Burlando, P. (2015). Storm type effects on super clausius–clapeyron scaling of intense rainstorm properties with air temperature. *Hydrology and Earth System Sciences*, *19*(4), 1753–1766. Retrieved from `https://hess.copernicus.org/articles/19/1753/2015/` doi: 10.5194/hess-19-1753-2015

Oki, T., & Sud, Y. C. (1998). Design of total runoff integrating pathways (trip)—a global river channel network. *Earth Interactions*, *2*(1), 1 - 37.

Papalexiou, S. M., & Montanari, A. (2019). Global and regional increase of precipitation extremes under global warming. *Water Resources Research*, *55*(6), 4901-4914.

Pendergrass, A. G., Lehner, F., Sanderson, B. M., & Xu, Y. (2015). Does extreme precipitation intensity depend on the emissions scenario? *Geophysical Research Letters*, *42*(20), 8767-8774.

Poujol, B., Sobolowski, S., Mooney, P., & Berthou, S. (2020). A physically based precipitation separation algorithm for convection-permitting models over complex topography. *Quarterly Journal of the Royal Meteorological Society*, *146*(727), 748-761.

Primo, C., Kelemen, F. D., Feldmann, H., Akhtar, N., & Ahrens, B. (2019). A regional atmosphere–ocean climate system model (cclmv5.0clm7-nemov3.3-nemov3.6) over europe including three marginal seas: on its stability and performance. *Geoscientific Model Development*, *12*(12), 5077–5095.

Purr, C., Brisson, E., & Ahrens, B. (2019). Convective Shower Characteristics Simulated with the Convection-Permitting Climate Model COSMO-CLM. *Atmosphere*, *10*(12).

Purr, C., Brisson, E., & Ahrens, B. (2021). Convective rain cell characteristics and scaling in climate projections for germany. *International Journal of Climatology*, *41*(5), 3174-3185.

Rasp, S., Selz, T., & Craig, G. C. (2016). Convective and slantwise trajectory ascent in convection-permitting simulations of midlatitude cyclones. *Monthly Weather Review*, *144*(10), 3961 - 3976.

Riahi, K., van Vuuren, D. P., Kriegler, E., Edmonds, J., O'Neill, B. C., Fujimori, S., ... Tavoni, M. (2017). The shared socioeconomic pathways and their energy, land use, and greenhouse gas emissions implications: An overview. *Global Environmental Change*, *42*, 153-168.

Rockel, B., Will, A., & Hense, A. (2008, 08). The regional climate model cosmo-clm (cclm). *Meteorologische Zeitschrift*, *17*(4), 347-348.

Rudolf, B., & Rapp, J. (2002). Das Jahrhunderthochwasser der Elbe: Synoptische Wetterentwicklung und klimatologische Aspekte. *DWD Klimastatusbericht*, 172–187.

Ruff, F., & Pfahl, S. (2023). What distinguishes 100-year precipitation extremes over central european river catchments from more moderate extreme events? *Weather and Climate Dynamics*, *4*(2), 427–447.

Ruti, P. M., Somot, S., Giorgi, F., Dubois, C., Flaounas, E., Obermann, A., ... Vervatis, V. (2016). Med-cordex initiative for mediterranean climate studies. *Bulletin of the American Meteorological Society*, *97*(7), 1187 - 1208.

Sodemann, H., Wernli, H., & Schwierz, C. (2009). Sources of water vapour contributing to the elbe flood in august 2002—a tagging study in a mesoscale model. *Quarterly Journal of the Royal Meteorological Society*, *135*(638), 205-

223.

Stein, C., & Malitz, G. (2013). Das Hochwasser an Elbe und Donau im Juni 2013. *Deutscher Wetterdienst*.

Stucki, P., Froidevaux, P., Zamuriano, M., Isotta, F. A., Messmer, M., & Martynov, A. (2020). Simulations of the 2005, 1910, and 1876 vb cyclones over the alps – sensitivity to model physics and cyclonic moisture flux. *Natural Hazards and Earth System Sciences*, *20*(1), 35–57.

Tandon, N. F., Zhang, X., & Sobel, A. H. (2018). Understanding the dynamics of future changes in extreme precipitation intensity. *Geophysical Research Letters*, *45*(6), 2870-2878.

Tiedtke, M. (1989). A comprehensive mass flux scheme for cumulus parameterization in large-scale models. *Monthly Weather Review*, *117*(8), 1779 - 1800.

Totz, S., Tziperman, E., Coumou, D., Pfeiffer, K., & Cohen, J. (2017). Winter precipitation forecast in the european and mediterranean regions using cluster analysis. *Geophysical Research Letters*, *44*(24), 12,418-12,426.

Tremblay, A. (2005). The stratiform and convective components of surface precipitation. *Journal of the Atmospheric Sciences*, *62*(5), 1513 - 1528.

Ulbrich, U., Brücher, T., Fink, A., Leckebusch, G., Krü, A., & Pinto, J. (2003, 10). The central European floods of August 2002: Part 1 Rainfall periods and flood development. *Weather*, *58*, 371-377.

van Bebber, W. (1891). *Die zugstrassen der barometrischen minima nach den bahnenkarten der deutschen seewarte für den zeitraum 1875-1890*.

Wilks, D. S. (2011). *Statistical methods in the atmospheric sciences* (Vol. 100). Academic press.

Figure 1.

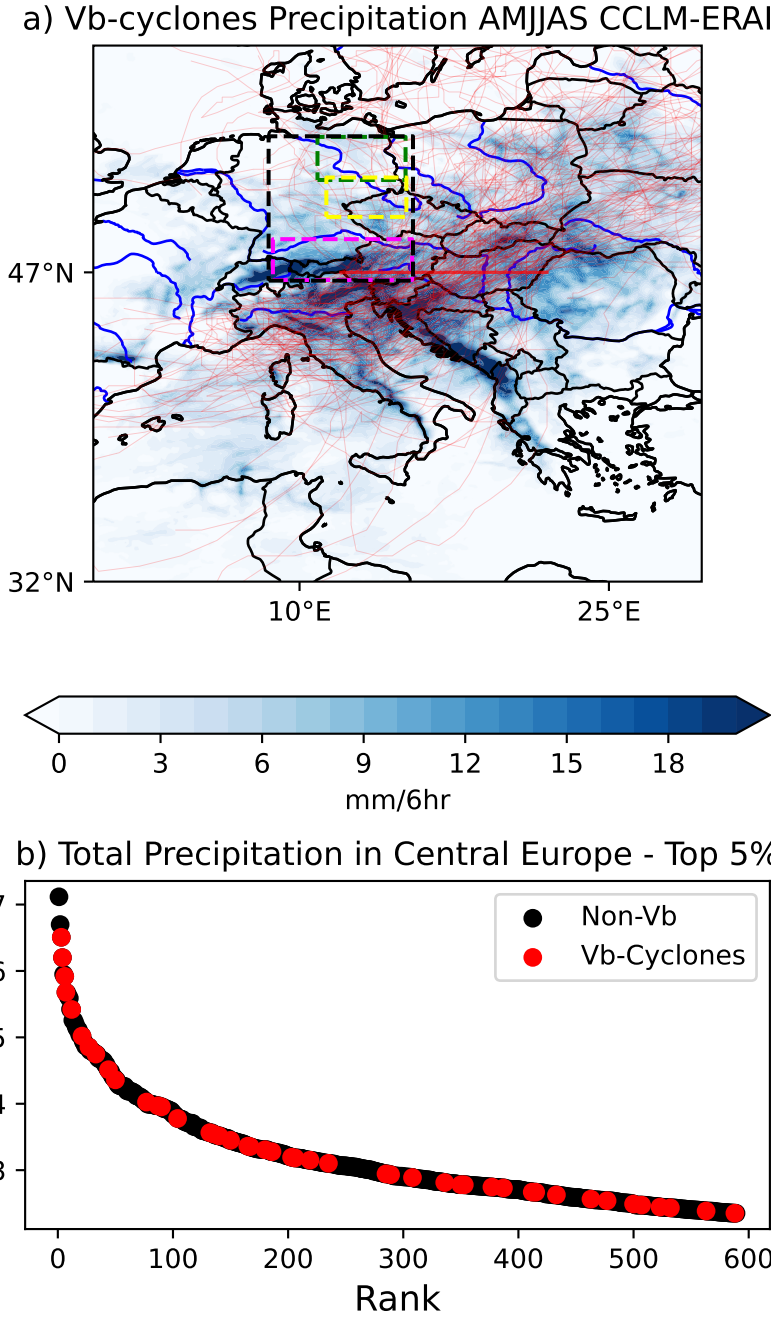
a) Vb-cyclones Precipitation AMJJAS CCLM-ERAI
47°N
32°N
10°E
25°E
0
3
6
9
12
15
18
mm/6hr
b) Total Precipitation in Central Europe - Top 5%
Precipitatiton mm/day
Rank
Non-Vb
Vb-Cyclones
0
100
200
300
400
500
600
3
4
5
6
7

Figure 2.

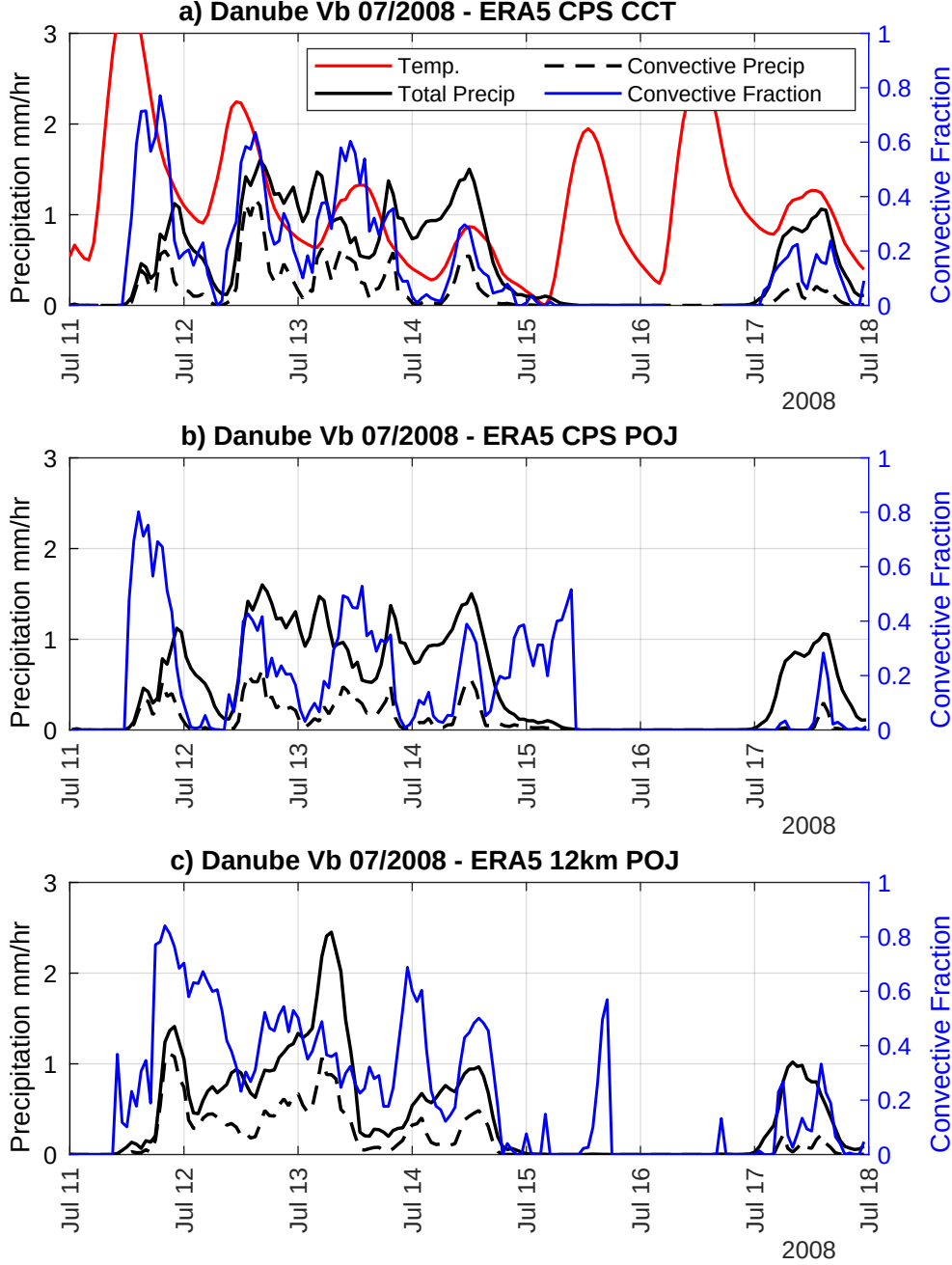
a) Danube Vb 07/2008 - ERA5 CPS CCT
Temp.
Total Precip
Convective Precip
Convective Fraction
Precipitation mm/hr
Convective Fraction
Jul 11
Jul 12
Jul 13
Jul 14
Jul 15
Jul 16
Jul 17
Jul 18
2008
b) Danube Vb 07/2008 - ERA5 CPS POJ
Precipitation mm/hr
Convective Fraction
Jul 11
Jul 12
Jul 13
Jul 14
Jul 15
Jul 16
Jul 17
2008
c) Danube Vb 07/2008 - ERA5 12km POJ
Precipitation mm/hr
Convective Fraction
Jul 11
Jul 12
Jul 13
Jul 14
Jul 15
Jul 16
Jul 17
Jul 18
2008

Figure 3.

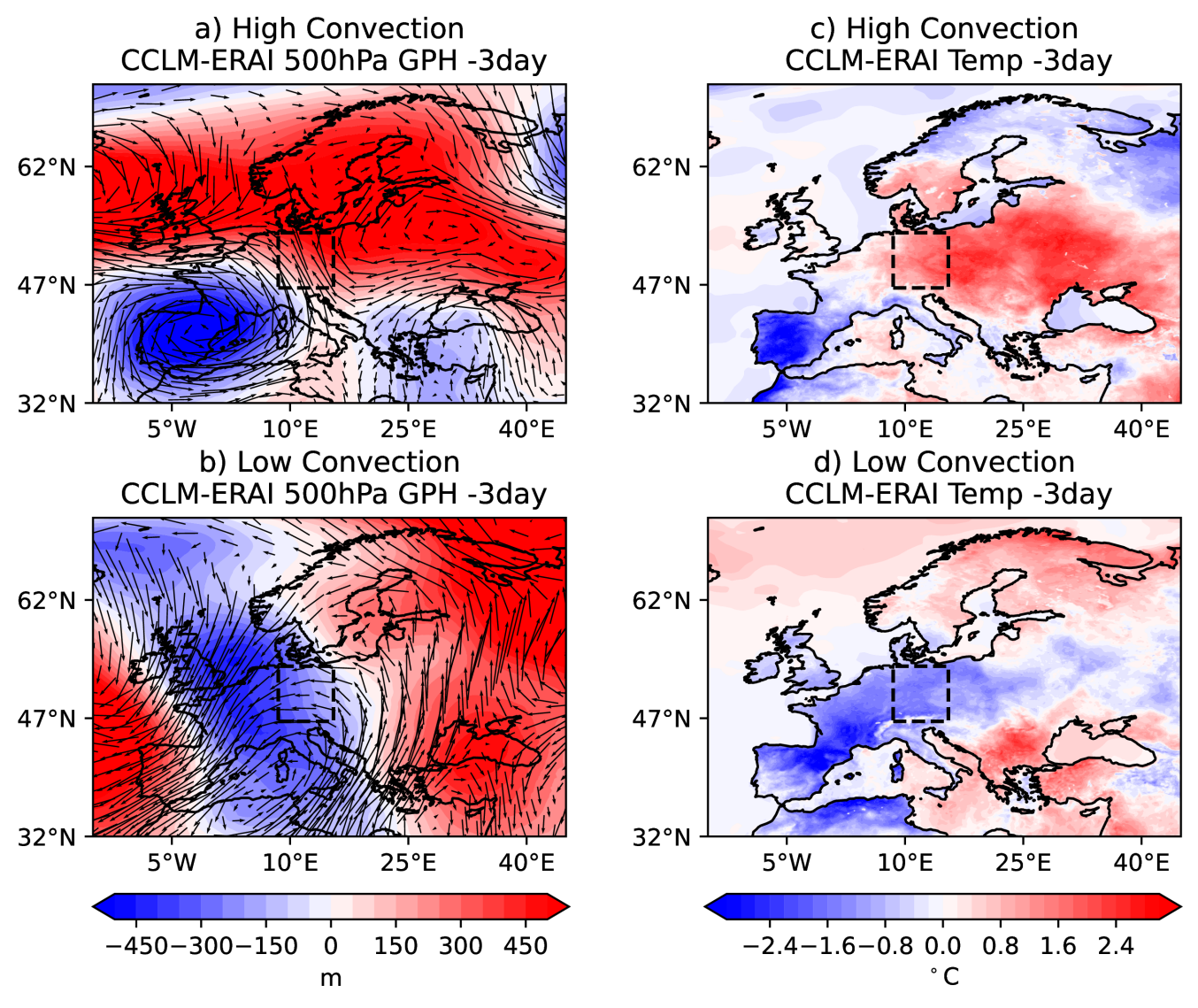
a) High Convection
CCLM-ERAI 500hPa GPH -3day
c) High Convection
CCLM-ERAI Temp -3day
b) Low Convection
CCLM-ERAI 500hPa GPH -3day
d) Low Convection
CCLM-ERAI Temp -3day
62°N
47°N
32°N
5°W
10°E
25°E
40°E
−450 −300 −150 0 150 300 450
m
−2.4 −1.6 −0.8 0.0 0.8 1.6 2.4
°C

Figure 4.

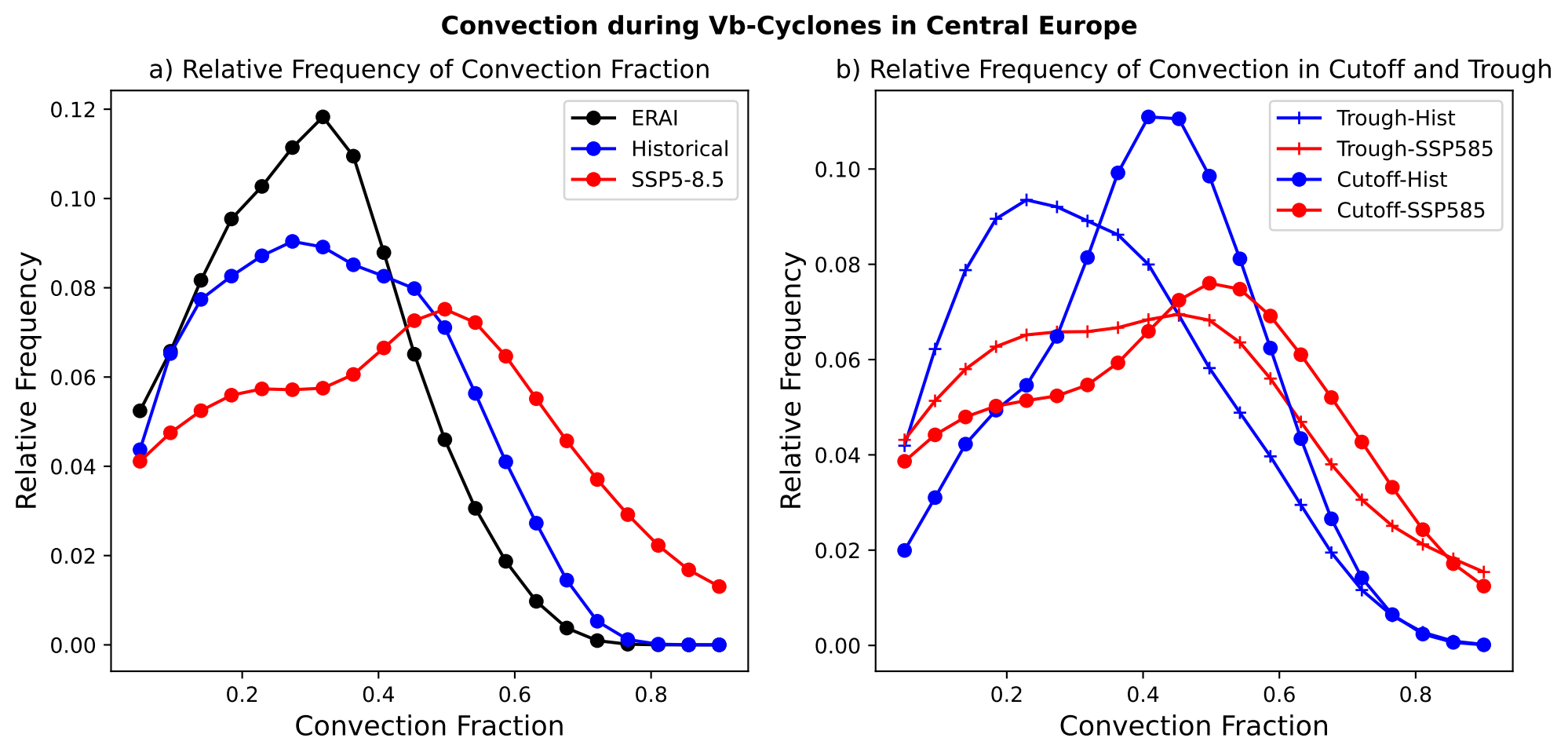
Convection during Vb-Cyclones in Central Europe
a) Relative Frequency of Convection Fraction
ERAI
Historical
SSP5-8.5
Relative Frequency
Convection Fraction
0.00
0.02
0.04
0.06
0.08
0.10
0.12
0.2
0.4
0.6
0.8
b) Relative Frequency of Convection in Cutoff and Trough
Trough-Hist
Trough-SSP585
Cutoff-Hist
Cutoff-SSP585
Relative Frequency
Convection Fraction
0.00
0.02
0.04
0.06
0.08
0.10
0.2
0.4
0.6
0.8